

THE MINERALOGY OF GLAUCONITE

GRAHAM R. THOMPSON

Department of Geology, University of Montana, Missoula 59801, U.S.A.

and

JOHN HOWER

Department of Geology, Case Western Reserve University, Cleveland, Ohio 44106, U.S.A.

(First received 22 February 1974; and in final form 6 February 1975)

Abstract—The mineral in monomineralic glauconite pellets is an iron-rich mixed-layer illite–smectite (here called glauconite), often composed almost entirely of illite layers. The nature of the interlayering is closely analogous to that of aluminous illite–smectite and varies with the proportions of the layer types: > 30 per cent smectite, randomly interstratified; 15–30 per cent smectite, allevardite-like ordering; < 15 per cent smectite, 'IMII' ordering.

Glauconite is analogous to aluminous illite–smectite chemically as well as structurally. A good correlation has been found between the number of potassium atoms per $O_{10}(OH)_2$ in structural formulas calculated from the chemical analyses and the proportion of illite layers as determined by X-ray powder diffraction methods. This relationship indicates a remarkably systematic increase in the potassium content of the illite layers with an increasing proportion of illite layers. This feature and the existence of ordered interlayering at high proportions of illite layers can be explained by crystal–chemical effects of illite layers on neighboring smectite layers. Glauconite differs from aluminous illite–smectite in that glauconite contains significantly less potassium per illite layer than does aluminous illite–smectite with the same proportion of illite layers except near the pure illite composition. The strength with which the interlayer potassium is held and the ease of conversion of smectite to illite layers in glauconite may be attributed to its IM structure and, perhaps, to its high octahedral iron content, which lead to stronger bonding of potassium by allowing a higher tilt angle of the O–H axis of hydroxyls adjacent to the potassium ion.

The apparent octahedral cation occupancy in excess of two-thirds of the octahedral positions in many glauconites appears largely attributable to the presence of significant amounts of interlayer hydroxy–iron, aluminum and magnesium complexes in the smectite layers.

INTRODUCTION

Since von Humboldt in 1823 (Schneider, 1927) originally described glauconite pellets in sedimentary rocks, many workers have studied its mineralogy and petrology (the literature has been reviewed by McRae, 1972).^{*} Using modern analytical techniques such as X-ray powder diffraction, Warshaw (1957) and Burst (1958 a, b) made the first detailed studies of the mineralogy of glauconite pellets and observed that all green pellets found in sedimentary rocks are not mineralogically alike and in some cases single pellets consist of heterogeneous mineral mixtures. These observations were subsequently corroborated by a number of workers, e.g. Hower (1961), Pratt (1962), Ehlmann *et al.* (1962), Triplehorn (1966), Barackman (1964) and Bell and Goodell (1967). Warshaw (1957), Burst

(1958a) and Hower (1961), in addition, noted that most glauconite pellets are monomineralic and consist of a mineral structurally similar to mixed-layer illite–smectite, and that there is considerable variation from sample to sample in the proportions of illite and smectite layers.

The purpose of this study was to investigate the mineralogy of glauconite (i.e. the iron-rich illite–smectite which is most commonly the predominant or exclusive mineral in glauconite pellets). Over 100 samples of glauconite pellets were examined. Of these samples, 20 were selected for further study.

These were chosen for their monomineralic nature and the homogeneity of their mixed-layering. They were chemically analyzed for the major elements and examined by X-ray powder diffraction and other techniques. Sample occurrence data are given in Table 1.

THE STRUCTURE OF GLAUCONITE

The sections that follow contain our interpretation of the mineralogy of glauconite, based on X-ray powder diffraction, acid dissolution, thermogravimetric and chemical analysis.

X-ray powder diffraction methods

Glauconite pellets were gently broken with an agate mortar and pestle and further disaggregated

^{*} Terminology—As pointed out by McRae (1972), the terminology associated with glauconite is quite confusing. It would be convenient to have a distinct name, (e.g. George) for the iron-rich illite–smectite of all proportions of interlayering that is the dominant or exclusive mineral in most glauconite pellets. However, we do not. In this paper we will call it glauconite and use it in a mineralogical sense. When referring to samples in morphological or occurrence sense we will use the term 'glauconite pellets'. This does not seem to us to be the most convenient way, but is the best solution without inventing new terminology, which we abhor.

Table 1. Catalog of glauconite samples

Sample	Collecting Data
GT8-66	Cambrian: Gros Ventre fm., Wind River Canyon, Wyo. 18" above lowest glauconite unit in canyon; 4' below lenticular pebble cong.
G294	Ordovician, Basal Arenigian Stage: Scora brottat, Latorp, Sweden. 15' below surface (J. Obradovich*).
G3585	Mississippian: Basal Barnett fm., Marble Falls, Texas.
FGS1x	Pennsylvanian: Canadian Arctic Loc. #3 (F.G. Stehli).
G1392	Jurassic, Lower Oxfordian Stage: core from well near Weiheim, Germany. Outer portion of pellet removed by ultrasonic treatment (J. Obradovich).
GT4-66a	Same as GT4-66b. Inner Core of pellet only.
GT4-66b	Jurassic: Sundance fm., Thermopolis, Wyo. 30' below Morrison fm. contact. Outer rind of pellet only.
GT6-69	Cretaceous, Cenomanian Stage (UK-LK boundary): Bornholm Island, (R. Douglas).
JH63-3	Cretaceous: Taft Hill fm., Manchester Freeway Exit, Great Falls, Mont. Lowest glauconite zone in Taft Hill fm.
Moody a & b	Eocene: Moody's Branch fm., Riverside City Park, Jackson, Miss. 4' above the top of Middle Eocene (C. Rainwater). A: outer part of pellets; b: core of pellets.
W89-1	Eocene, Claiborne Stage: Winona fm. Northwestern Attala Co., Miss. (E. G. Wermund).
GT2-69	Eocene: Cayat fm., Lower Potrero Hills, Calif. (R. Douglas).
W89-6	Eocene, Claiborne Stage: Zilpha fm., Northwestern Attala Co., Miss. (E. G. Wermund).
W46	Eocene, Sabine Stage: Basal Nanafalia fm., Marengo Co., Ala. (E.G. Wermund).
W89-2	Same as W89-1, 3 "beds" higher in section (E.G. Wermund).
W87	Eocene, Claiborne Stage: Winona fm., Yalobusha Co., Miss. 3' above Tallahatta contact (E.G. Wermund).
G68A	Eocene, Claiborne Stage: Hurricane lentil in Landrum fm., Leon Co., Texas (E.G. Wermund).
6471	Recent: Lat. N36° 40' 56", Long. W122° 00' 00" (W. Pratt).
6433	Recent: Lat. N35° 41' 32", Long. W121° 53' 25" (W. Pratt).

ultrasonically. The clay suspensions were then mounted on unglazed ceramic tiles by the method of Kinter and Diamond (1956). Air-dried and ethylene-glycol solvated samples were run on a General Electric XRD-6 using $\text{CuK}\alpha$ radiation and scan speeds of 2° and 0.4° $2\theta/\text{min}$.

Reynolds and Hower (1970) have developed an analog computer program to synthesize X-ray powder diffraction patterns for mixed-layer illite-smectite of varying expandabilities and types of interlayering. Their published patterns show excellent correspondence to X-ray diffraction patterns of naturally occurring illite-smectite. To test the idea that glauconite is structurally similar to illite-smectite, this program has been used to calculate patterns for iron-rich illite-smectite of varying proportions of interlayering, types of ordering and crystallite thickness. Calculations were made using an iron content in the octahedral layer of 0.9 Fe atoms/ $0_{10}(\text{OH})_2$ which is typical of glauconite; other conditions were the same as those used by Reynolds and Hower.

Representative calculated X-ray powder diffraction patterns and representative X-ray powder diffraction patterns from samples of naturally occurring glauconite are shown in Fig. 1.

Interpretations of the X-ray patterns

As can be seen in Fig. 1, the correspondence between the calculated patterns and the patterns from

representative glauconite samples is excellent. The fact that the program, used to interpret the structure of illite-smectite, produces patterns matching those of natural glauconite, leads us to conclude that glauconite is structurally analogous to illite-smectite and that it is valid to draw detailed structural interpretations from comparison of the X-ray powder diffraction patterns of glauconite with the calculated diffraction profiles.

It is more difficult to make an accurate determination of the proportions of layers in glauconite than in illite-smectite because of the low intensity of the reflection that occurs between 15.6° and 17.7° 2θ ($\text{CuK}\alpha$). This reflection (the combined $(002)_{10\text{\AA}}/(003)_{17\text{\AA}}$ for random interstratification) is the most useful in the quantitative interpretation of patterns of illite-smectite, but is weak in those of glauconite because of the presence of large amounts of iron in the octahedral layer (see Grim *et al.*, 1951) for the effect of octahedral iron on $(00l)$ intensities of dioctahedral micas). The difference in relative peak intensity does not, of course, alter the structural interpretations; however, in the diffraction patterns of some glauconites the intensity of the $(002)_{10\text{\AA}}/(003)_{17\text{\AA}}$ reflection

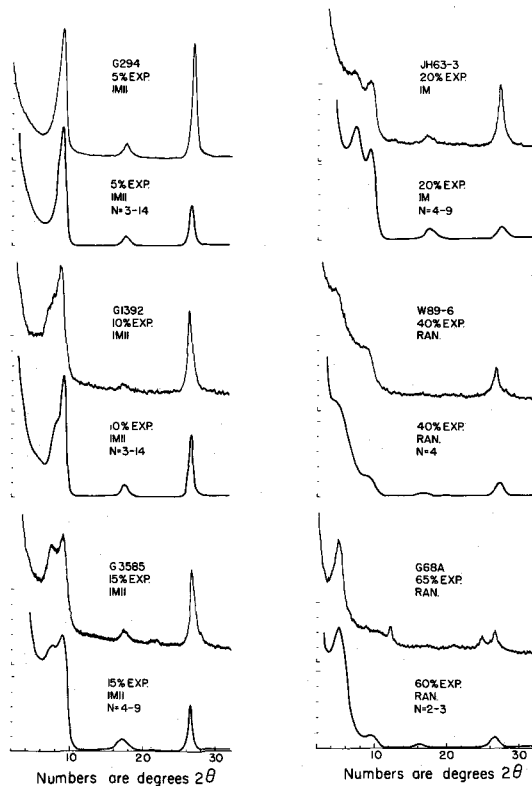


Fig. 1. Comparison of X-ray powder diffraction patterns of oriented, glycol solvated glauconite, with computer calculated diffraction profiles after the method of Reynolds and Hower (1970). The tracings labeled G294, G1392, G3585, JH63-3, W89-6, and G68A are actual patterns from glauconite samples; the profile immediately below each glauconite pattern is a calculated pattern. N = the range in number of layers per crystallite used in calculating the patterns. Interlayering type is either random (RAN), all-variant-ordered (IM), or ordered with an IMII superlattice. Sample G68A contains some 7 Å material.

is so low that its spacing cannot be determined with precision. In these cases one must rely on the shape and position of the low angle peaks, and the precision of estimating the proportions of layers is poorer. We estimate precision to be ± 5 per cent at low expandabilities, and ± 10 per cent at high expandabilities. The proportion of layers and the manner of interstratification of the glauconites examined in detail in this study are presented in Table 2. Figure 1 shows diffraction patterns of samples covering a large range of inter-layering.

Based on the interpretations shown in Table 2, supplemented by an examination of diffraction patterns of a large number of additional samples during the sample selection procedure, the following general observations regarding the nature of mixed-layering in glauconite can be made;

(1) glauconite structures range from those with fewer than 5 to more than 65 per cent smectite layers. Pratt (1962) has reported some recent glauconites which are composed of more than 65 per cent smectite layers,

(2) glauconites with more than 25–30 per cent smectite layers are randomly interstratified (Fig. 1; G89-6, G68A),

(3) most glauconites with 10 to 25 per cent smectite layers show alleverdite-like ordering (i.e. smectite layers are separated by at least one illite layer) (Fig. 1; JH-63-3),

(4) glauconites with less than 10 per cent (and a few with 15 per cent) smectite layers exhibit the type of ordering which Reynolds and Hower (1970) describe as the IMII type (Fig. 1; G294 and G3585) and

(5) even samples of glauconite pellets which, upon cursory examination, appear monomineralic often show minor mineral impurities on detailed analysis. This is particularly true of the more expandable samples, although a mixture of a small amount of 10 \AA impurity in samples of low expandability would be undetectable in the X-ray diffraction patterns.

CHEMICAL COMPOSITION OF GLAUCONITE

Analytical techniques

The elements silicon, aluminum, iron, titanium, calcium and potassium were quantitatively determined in 21 samples by vacuum X-ray emission spectrometry. Matrix corrections were made using a computer program modified from that of Hower *et al.* (1965). Prior to analysis the samples were heated at 1000°C for three hr to remove absorbed and structural water, diluted 2:1, 4:1, or 9:1 (depending upon abundance of sample) with $\text{Li}_2\text{B}_4\text{O}_7$ and fused to minimize matrix effects; the fused samples were ground and pressed into pellets for analysis. A standard, which approximated the composition of glauconite, was made from oxides of the metals. Standard deviation, in terms of per cent of the amount present, are; iron ± 1.02 per cent, titanium ± 2.74 per cent, potassium ± 1.30 per cent, calcium ± 3.69 per cent, silicon

Table 2. Structural characteristics of glauconite samples

Sample	Percent Smectite	Type of Ordering	Remarks
G294	5	IMII	heterogeneous expandability between 15% and 20%
GT8-66	5-10	IMII	
FGS1x	10	IMII	
G1392	10	IMII	
GT6-69	10	IMII	
G3585	15	IMII	
GT4-66b	15	IMII	
Moody b	15-20	IM	
GT4-66a	20-25	IM	
JH63-3	20	IM	
W46	30-35	Random	contains some 7 \AA and some discrete 10 \AA
GT2-69	35	Random	
W89-2	35-40	Random	
W89-6	40	Random	
6433	40	Random	
W87	40-45	Random	
6471	45	Random	
Moody a	50	Random	
G68A	65	Random	

± 1.01 per cent, and aluminum ± 2.89 per cent. Seven \AA mineral impurities were removed prior to chemical analysis by heat treatment and base dissolution as described by Brown (1961). Samples with more than very minor amounts of other impurities were not chemically analyzed. Sodium content was determined using a flame photometer. Ferrous:ferric ratios were determined by the method of Reichen and Fahey (1962). Sodium contents and ferrous:ferric ratios were not determined on a few samples for which there was insufficient material. The chemical analyses are reported in Table 3.

STRUCTURE—COMPOSITION RELATIONSHIPS IN GLAUCONITE

The chemical composition of glauconite varies over a wide range. This range, as determined from this study and analyses published by other workers (Hendricks and Ross, 1941; Burst, 1958), is summarized in Table 4.

Compositional variations in the mixed-layer series

The chemical analyses in Table 3 have been re-cast into structural formulas based on a cell with an anion content of $\text{O}_{10}(\text{OH})_2$ and are shown in Table 5. The structural formulas were calculated by ignoring the sodium and calcium and assuming that the cation exchange capacity is 8 m-equiv./100 g/10 per cent smectite layers (Manghnani and Hower, 1963). This approach was taken because a few samples were slightly contaminated with calcite and, for some samples, insufficient material was available for a sodium analysis. In this way the formulas are calculated on a uniform basis. Pure samples with sodium analyses yielded identical structural formulas when the formulas were calculated either assuming a cation exchange capacity or by including sodium in the calculations.

As with normal illite-smectites (Hower and Mowatt, 1966), it would be expected that in glauconite the number of potassium atoms (K_n) per $\text{O}_{10}(\text{OH})_2$ would increase with the proportion of illite layers (cf. Table 2). The relationship is excellent (Fig. 2) but cannot be interpreted simply, because the curve increases

Table 3. Chemical analyses of glauconite specimens in weight per cent of oxide (water-free)

	GT8-66	G294	GT6-69	G1392	FGSLx	G3585	Moody b
SiO ₂	53.13	56.98	54.94	53.91	57.49	59.31	53.51
TiO ₂	0.17	0.08	0.08	0.18	0.20	0.36	0.97
Al ₂ O ₃	10.35	13.33	9.53	13.34	9.37	14.40	13.61
Fe ₂ O ₃	21.70	8.78	17.86	21.08	17.46	12.05	16.67
FeO	1.74	7.05	1.97	0.61	4.62	1.38	3.17
MgO	3.43	5.35	4.77	3.61	1.79	6.93	5.56
CaO	0.15	0.05	0.72	0.07	0.08	0.19	0.31
Na ₂ O	0.20	0.23	0.18	0.39	0.13	0.19	0.13
K ₂ O	8.50	8.21	7.82	7.62	7.16	6.68	5.60
Total Percentage	99.56	100.84	98.09	100.18	98.81	101.64	99.88
Percent Smectite Layers	5-10	5	10	10	10	15	15-20

	GT4-66b	JH63-3	GT4-66a	W89-1	GT2-69	W89-6
SiO ₂	58.26	57.63	55.16	59.18	55.53	58.54
TiO ₂	0.52	0.33	0.66	0.24	0.43	0.29
Al ₂ O ₃	14.31	16.22	16.71	14.32	15.55	12.71
Fe ₂ O ₃	15.29	10.66	17.24	16.61	13.02	19.46
FeO	2.30	2.02	-	-	3.74	-
MgO	1.91	3.66	4.07	4.41	3.64	2.20
CaO	0.18	1.10	0.05	0.02	0.12	0.02
Na ₂ O	0.28	0.24	-	-	3.50	-
K ₂ O	5.02	4.99	4.75	4.73	4.36	3.98
Total Percentage	98.33	97.07	98.64	99.51	98.89	97.20
Percent Smectite Layers	15	20	20-25	n.d.	35	40

	W46	W89-2	6471	6433	W87	G68a
SiO ₂	58.45	57.71	57.40	56.88	55.49	54.89
TiO ₂	0.53	0.45	0.95	0.79	0.41	0.74
Al ₂ O ₃	14.38	16.43	12.16	11.57	18.24	18.62
Fe ₂ O ₃	16.61	15.74	10.11	10.79	11.02	14.92
FeO	--	--	6.72	5.70	3.76	0.14
MgO	2.26	1.57	4.78	6.25	2.18	5.39
CaO	0.09	0.01	0.42	2.13	0.04	0.97
Na ₂ O	--	--	3.91	3.85	0.08	0.27
K ₂ O	3.78	3.66	2.56	2.55	2.28	1.81
Total Percentage	96.10	95.57	99.01	100.51	93.92	97.77
Percent Smectite Layers	30-35	35-40	45	40	40-45	65

in slope with an increasing proportion of illite layers. The shape and position of the curve indicates that the mean potassium content of the illite layers in a glauconite with a highly expandable structure is very low and that the mean potassium content per illite layer increases as the proportion of illitic layers increases. This change is readily seen by calculating the number of potassium atoms per O₁₀(OH)₂ in the illite portion of the structure (cf. Weaver, 1965). For example, the curve passes through K_n = 0.12 at 40 per cent illite layers; the number of potassium atoms per O₁₀(OH)₂ in the illite of the structure is thus K_n/0.4 = 0.12/0.4 = 0.30. This value is quite different from either that of an ideal mica (1.0 K/O₁₀(OH)₂) or of an illite with no smectite interlayering (about

0.8 K/O₁₀(OH)₂, Hower and Mowatt, 1966). The mean potassium content of the illite layers has been calculated in the same manner for differing proportions of illite layers and is presented in Table 6. It can be seen that as glauconite approaches 100 per cent illite layers the number of potassium atoms per O₁₀(OH)₂ in the illite layers approaches that of aluminous illites. A comparison of the relationship between K_n and percent illite layers in glauconite and aluminous illite-smectite is shown in Fig. 2. The curve for aluminous illite-smectite is from Hower and Mowatt (1966). The curves are obviously quite different. However, aluminous illite-smectites also show, although to a lesser extent, an increasing number of potassium atoms per O₁₀(OH)₂ in the illite layers that

Table 4. Range in chemical composition of glauconite

Oxide	Maximum - Source		Minimum - Source	
K ₂ O	9.01	a	1.81	b
SiO ₂	59.31	b	41.02	a
Al ₂ O ₃	23.6	c	1.52	a
Total Fe as Fe ₂ O ₃	31.09	a	7.26	a
Fe ₂ O ₃	27.98	a	6.17	a
FeO	8.00	c	0.14	b
Fe ³ /Fe ²	90.60	b	1.12	b
Mg	6.93	b	0.57	a
Na ₂ O	3.91*	b	0.00	a and c
CaO	3.95*	a	0.00	c

a Hendricks and Ross (1941)

b This study

c Burst (1958a)

* High value may be due to undetected impurities

is displayed so strikingly by the iron-rich illite-smectite of glauconite (Table 6).

The formation of illite layers and ordering of mixed-layering

We believe that the systematic variation in potassium content of the illite layers and the existence of allevardite-like ordering in structures with a high proportion of illite layers in the illite-smectite series have a common explanation. This explanation can be most readily understood by considering the progressive conversion of a completely expandable smectite into an illite through the mixed-layer series and is based on Sawhney's (1967) interpretation of the formation of ordered biotite-vermiculite in the conversion of vermiculite to biotite in laboratory alteration experiments.

According to Sawhney (1967) ordered interlayering

Table 5. Structural formulas of glauconite specimens: number of cations per O₁₀(OH)₂, octahedral occupancy and lattice charge

Position	Ion	GT8-66	G294	GT6-69	G1392	FGS1x	G3585	Moody b	JH 63-3	GT 4-66b	GT4-66a
Tetrahedral	Si	3.62	3.76	3.75	3.57	3.89	3.84	3.57	3.80	3.83	3.59
	Al	0.38	0.24	0.25	0.43	0.11	0.16	0.43	0.20	0.17	0.41
	Charge	-0.38	-0.24	-0.25	-0.43	-0.11	-0.16	-0.43	-0.20	-0.17	-0.41
Octahedral	Al	0.45	0.80	0.52	0.61	0.64	0.77	0.64	1.06	0.94	0.87
	Fe ⁺³	1.11	0.44	0.92	1.05	0.89	0.59	0.84	0.53	0.76	0.84
	Fe ⁺²	0.10	0.39	0.11	0.03	0.26	0.07	0.18	0.11	0.12	*
	Mg	0.35	0.53	0.49	0.36	0.18	0.67	0.55	0.36	0.18	0.40
	Sum	2.01	2.16	2.04	2.05	1.97	2.10	2.21	2.06	2.00	2.11
	Charge	-0.42	-0.44	-0.48	-0.24	-0.53	-0.44	-0.10	-0.27	-0.30	-0.07
	Total Lattice Charge	-0.80	-0.68	-0.73	-0.67	-0.64	-0.60	-0.53	-0.47	-0.47	-0.48
Interlayer	K	0.74	0.69	0.68	0.64	0.62	0.55	0.48	0.42	0.42	0.40
	X ⁺¹	0.03	0.02	0.03	0.03	0.03	0.05	0.06	0.06	0.05	0.07
	Inter-layer Charge	+0.77	+0.71	+0.71	+0.67	+0.65	+0.60	+0.54	+0.48	+0.47	+0.47
	CEC (estimated from % smectite) MEQ/100 gms	6	4	8	8	8	12	14	16	12	18

Position	Ion	W89-1	CT2-69	W89-6	W46	W89-2	6433	6421	G87	G68A
Tetrahedral	Si	3.76	3.69	3.83	3.84	3.79	3.84	3.87	3.71	3.55
	Al	0.24	0.31	0.17	0.16	0.21	0.16	0.13	0.29	0.45
	Charge	-0.24	-0.31	-0.17	-0.16	-0.21	-0.16	-0.13	-0.29	-0.45
Octahedral	Al	0.83	0.91	0.81	0.95	1.06	0.76	0.84	1.15	0.97
	Fe ^{#3}	0.79	0.65	0.96	0.82	0.78	0.55	0.51	0.55	0.72
	Fe ⁺²	*	0.21	*	*	*	0.32	0.38	0.21	0.01
	Mg	0.42	0.36	0.22	0.22	0.15	0.64	0.48	0.21	0.52
	Sum	2.04	2.13	1.99	1.99	1.99	2.27	2.21	2.12	2.22
	Charge	-0.30	-0.18	-0.25	-0.25	-0.18	0.15	0.23	-0.06	+0.13
	Total Lattice Charge	-0.54	-0.49	-0.42	-0.41	-0.39	-0.31	-0.36	-0.35	-0.32
Interlayer	K	0.38	0.37	0.33	0.32	0.31	0.22	0.22	0.19	0.15
	X ⁺¹	0.12	0.11	0.13	0.10	0.12	0.13	0.15	0.14	0.20
	Inter-layer Charge	+0.50	+0.48	+0.46	+0.42	+0.43	+0.35	+0.37	+0.33	+0.35
	CEC (Estimated from percent smectite) MEQ/100 gms	32	28	32	26	30	32	36	34	51

* not determined

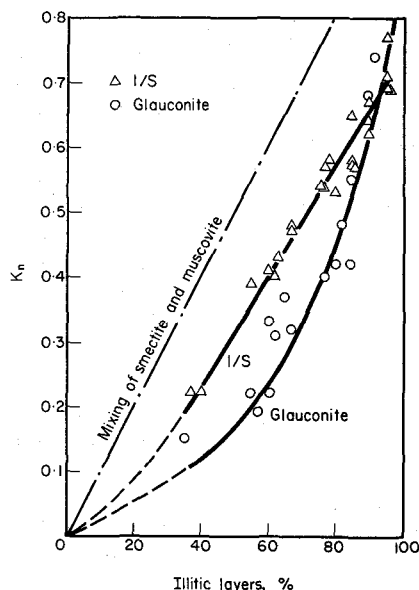


Fig. 2. Relationships between the number of potassium atoms per $O_{10}(OH)_2$ (K_n) and the percent illite layers in glauconite and in aluminous illite-smectite.

of hydrated and non-hydrated interlayers occurs during the replacement of Ca^{2+} by K^+ in vermiculite because the contraction of a layer to 10 \AA reduces the effective interlayer charge available to the adjacent (hydrated) interlayer spaces, thus making the latter less likely to contract. The reduction of effective interlayer charge in the adjacent hydrated layers results from the polarization of electronic charge within the 2:1 layers in the direction of the dehydrated interlayer space, caused by the shortening of the interlayer cation-oxygen bonds on loss of interlayer water and a concomitant reduction in the dielectric constant of the dehydrated interlayer space.

If we now consider the progressive conversion of a smectite to an illite it can be seen that the same mechanism should operate. The first layers to contract should be able to do so even when there is a relatively low charge on the adjacent 2:1 layers and a relatively low interlayer potassium content. The hydrated interlayer spaces adjacent to the contracted interlayer would then need a greater amount of substitution in the flanking tetrahedral and octahedral layers and a higher potassium content before they would be able to contract. Therefore as the number of illite layers increases, further illite layer formation demands a higher substitution within bounding 2:1

Table 6. Mean number of potassium atoms per $O_{10}(OH)_2$ in the illite layers of glauconite and aluminous illite-smectite for differing proportions of illite layers

% Illite Layers	Glauconite	Illite/Smectite
40	0.30	0.58
50	0.34	0.63
60	0.39	0.67
70	0.46	0.70
80	0.56	0.72
90	0.69	0.74

layers and a higher potassium content. This accounts for the K_n vs per cent illite layers relationship shown in Fig. 2.

The above explanation also accounts in a qualitative sense for the presence of ordering in illite-smectite and glauconite with a high proportion of illite layers. The model predicts complete allevardite ordering when the proportion of illite layers reaches 50 per cent. Aluminous illite-smectite becomes completely ordered when 60-65 per cent of the layers are illite, and glauconite when about 70 per cent of the layers are illite (cf. Table 2). We suggest that partial ordering begins when the proportion of illite layers is less than 60-70 per cent in both of these series, but that ordering does not become sufficiently developed to be detectable by X-ray powder diffraction methods until a higher level of illite content is attained.

Mineralogical differences between illite-smectite and glauconite

As can be seen from Fig. 2 and Table 6 the potassium content of illite layers in highly expandable glauconite is far lower than it is in aluminous illite-smectite with the same structure. We believe that the formation of illite layers in a glauconite structure containing a high proportion of smectite layers at a low potassium content can be attributed to its 1M structure and additionally, perhaps, to the presence of large amounts of iron in the octahedral layer. The explanation is based on the influence of structure and composition on the proximity of the hydrogen on the hydroxyl ion of the 2:1 structure to the adjacent potassium ion in micas.

Our argument follows from the explanation first outlined by Bassett (1960) to account for the fact that trioctahedral micas are more easily converted to vermiculite by leaching with such ions as Mg^{2+} than are dioctahedral micas. Bassett's i.r. absorption analyses indicated that in phlogopite the orientation of the O-H axis of the hydroxyl immediately adjacent to the potassium ion is normal to the (001), being forced there by electrostatic repulsion of the symmetrically disposed magnesium ions in the octahedral sites. By contrast, the vacancies in the octahedral layer of dioctahedral micas allows the O-H axis to tilt away from the potassium ions toward the octahedral vacancies (Tsuboi, 1950; Vedder and McDonald, 1963; Bassett, 1960). Giese's (1971) electrostatic energy calculations of the muscovite structure indicate that the tilt of the 72° of the O-H axis with respect to the normal to the (001) is quantitatively explained by electrostatic response to the surrounding ions. Bassett's explanation of the ease of the interlayer alteration of phlogopite as compared to muscovite is that the potassium ion in phlogopite is less strongly bonded than is potassium in muscovite because of electrostatic repulsion by the hydrogen which is situated closer to the potassium ion in the phlogopite than in the muscovite structure. Giese (1973) has further shown that the amount of tetrahedral rotation should strongly in-

fluence the tilt of the O–H axis and, on the basis of published structures, has calculated maximum O–H axis tilt (90°) for the 1M structure. Glauconite is a 1M polymorph (Burst, 1958b) and should thus provide this most stable bonding environment for the interlayer potassium. In addition, although intuitive reasoning does not always lead to the correct answer in dealing with questions concerning the balance of electrostatic forces in a structure as complicated as a mica (Giese, personal communication, 1973), it seems to us that the higher electronegativity of iron as compared to aluminum would allow an even greater tilt of the O–H axis into the octahedral vacancy in glauconite than in an aluminous dioctahedral 1M structure.

Excess octahedral occupancy in glauconite

Although glauconite is generally considered to have a dioctahedral structure (cf. Burst, 1958) some authors (Yoder, 1959; Bentor and Kastner, 1965) have suggested that there may be a certain amount of 'trioctahedral character,' caused by some substitution of $3R^{2+}$ for $2R^{3+}$ in the octahedral layer. Their suggestions arise from the fact that when structural formulas are calculated (assuming an anion content of the cell of $O_{10}(OH)_2$, Marshall, 1935) the number of octahedral cations that results is sometimes significantly greater than the ideal 2.00. This feature is shown by a number of the formulas listed in Table 5. The range of calculated numbers of octahedral cations is 1.97–2.27. Because of the vagaries of analytical techniques and the assumptions made in calculating the formulas, we consider 2.00 ± 0.05 to be not significantly different from dioctahedral. There remain nine of the nineteen formulas in Table 5 that indicate excess octahedral occupancy.

A number of possibilities exist that could explain the apparent excess in the number of octahedral cations. For example, Foster (1951) showed that montmorillonites reported to have octahedral occupancies as high as $2.2/O_{10}(OH)_2$ contain exchangeable magnesium which, when assigned to the interlayer site, reduced the calculated octahedral occupancy to 2.00 ± 0.02 . Although there certainly may be some exchangeable magnesium in our samples, this explanation is not sufficient because formulas adjusted to 2.00 octahedral cation per $O_{10}(OH)_2$ yield unrealistically high interlayer charges (greater than 1 equiv./ $O_{10}(OH)_2$) for the smectite layers. As outlined below, it appears as if the presence of interlayer hydroxy complexes of iron, magnesium and aluminum explains the apparent excess octahedral occupancy in a more satisfactory manner. The existence of these interlayer hydroxy-metal complexes was determined by techniques of progressive acid dissolution, thermogravimetric analysis and thermal X-ray diffraction.

Techniques of progressive acid dissolution analysis

The technique of progressive acid dissolution analysis is based on the fact that cations occupying

different structural sites in a mineral are extracted at different rates when the mineral is leached with an acid solution. By analyzing the rates at which ions are extracted from a sample, it is possible to interpret how much of each ion is present in different structural and extrastructural sites in a crystal lattice and in which sites the ions are bonded. The technique has been used by a number of workers to determine cation distribution in layer silicates (e.g. Brindley and Youell, 1951; Osthaus, 1954, 1956; Granquist and Sumner, 1957; Cloos *et al.*, 1960; Ross, 1969).

The acid dissolution technique used in this study involved stirring a known quantity of disaggregated glauconite sample in a known volume of dilute HCl at a constant temperature. The acid was sampled at frequent intervals and aliquots were analyzed for the ions under consideration.

Previous studies (Osthaus, 1954, 1956; Granquist and Sumner, 1957) have established that acid dissolution of specific ions in layer silicates obeys first order rate laws. This means that the extraction rate, expressed as the rate of change of concentration of the ion under consideration remaining in the glauconite, is constant. When the log of the concentration is plotted against time, a straight line results for a first order reaction. If an ion is bonded in two different lattice sites the ion will generally be removed at two different rates and a plot of log concentration vs time will be the sum of the two linear extraction rates and will appear as a curve. When such a curve results, it can be deconvolved (*i.e.* separated into extraction rates for the ion from each bond site) by subtracting the contribution by the site with the lowest rate and plotting the remainder on another log concentration vs time curve. This is done by extrapolating the linear portion of the curve at long times (where the contribution of the higher rate curve is insignificant) back to zero and subtracting this from the total curve. If more than two solution rates exist, the process can theoretically be continued to complete deconvolution. The amount of the ion in each bond site is also given by the deconvolution.

This technique is well-suited to an attempt to determine whether some of the ions which are identified by standard structural formula calculations as being octahedrally coordinated in the 2:1 portion of the structure of glauconite may, in fact, actually be bonded in some other way in the glauconite lattice, or be extraneous to the structure.

Results of progressive acid dissolution analyses

Progressive acid dissolution studies were made for the standard octahedrally coordinate cations in glauconite (magnesium, aluminum and iron) for two samples (G294 and G68A) which showed an octahedral occupancy of 2.16 and 2.22, respectively. Extraction rates for potassium were also determined for these samples. Potassium results will be discussed in a later section. The results of the progressive acid dissolution studies for samples G294 and G68A are shown in Figs. 3 and 4. It is readily apparent that both G294

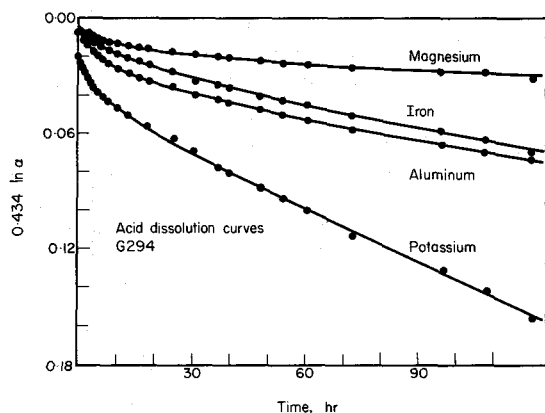


Fig. 3. Acid dissolution curves for magnesium, iron, aluminum and potassium for sample G294. α = fraction of elements remaining in solid.

and G68A contain significant amounts of iron, aluminum, and magnesium that are rapidly removed by acid attack and that extraction rates reach constant values in each series. Therefore it is possible to extrapolate the linear portions of the curves back to time zero and to determine the amounts of rapidly removed iron, aluminum, and magnesium for each sample. The results of this determination are shown in Table 7.

The linear portion of each curve is interpreted as reflecting the rate of extraction of each ion coordinated in the octahedral site in the 2:1 portion of the structure. (This is not strictly true for aluminum, of course, as some aluminum is bonded in tetrahedral as well as octahedral sites). The fact that a significant amount of each ion is removed at a rate considerably higher than the extraction rate for the octahedrally coordinated ion implies that each sample contains a significant amount of iron, aluminum and magnesium which is not coordinated in octahedral sites in the 2:1 portion of the structure, but rather is bonded in some kind of a site or sites from which it is much more easily removed. Some of this more easily removed material is extracted rapidly enough to be considered exchangeable. However, most of the rapidly extracted iron, aluminum and magnesium is

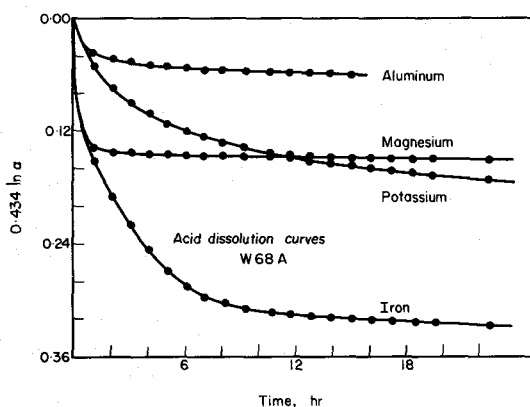


Fig. 4. Acid dissolution curves for magnesium, iron, aluminum and potassium for sample G68A. α = fraction of element remaining in solid.

not present as exchange ions. The thermogravimetric and thermal X-ray diffraction data presented below strongly suggest that the bulk of the rapidly extracted iron, aluminum and magnesium is present as inter-layer hydroxy-complexes in the glauconites which show apparent excess octahedral occupancy.

Thermogravimetric analysis

In the past few years, several workers have commented upon the presence of hydroxy-complexes of iron, magnesium, and aluminum in the interlayer spaces of expandable layer silicates (e.g. Rich, 1968; Slaughter and Milne, 1960; Gupta and Malik, 1969a, 1969b). We used thermogravimetric analysis (TGA) to attempt to establish whether the quantities of iron, aluminum and magnesium, determined in the previous section not to be coordinated in octahedral sites in the 2:1 portion of the structure, might be present as hydroxy complexes of these ions in the glauconite samples which show apparent excess octahedral occupancy.

Three glauconite samples, two of which show excess octahedral occupancy and one which approaches the ideal of two octahedral cations per unit cell, were subjected to TGA. A nitrogen atmosphere was used so that oxidation of Fe^{2+} would not occur and alter weight loss curves. TGA curves are shown in Fig. 5. The smectite curve (from Schultz, 1971) shows two major episodes of weight loss, one in the temperature interval from 20 to about 120°C and the other from 520 to 700°C. Schultz interpreted the first interval as loss of interstitial, adsorbed and interlayer water and the second as reflecting dehydroxylation of the 2:1 octahedral layer. He attributed the small weight loss between 130–520°C to a combination of the slow loss of a small amount of trapped interlayer water and the beginning of dehydroxylation.

The ideally dioctahedral glauconite GT8-66 shows a weight loss from room temperature to about 140°C. This weight loss is readily interpretable as loss of interstitial adsorbed and interlayer water, the amount of which is much less than in the smectite because GT8-66 is a structure of much lower expandability. The second weight loss event occurs between 350 and 700°C. This, by analogy with the smectite, is dehydroxylation of the octahedral layer. Dehydroxylation begins at a lower temperature in glauconite than in aluminous smectite because of the presence of octahedral Fe^{3+} and Fe^{2+} and parallels the relative thermal behavior of biotite (MacKenzie, 1970). The weight loss from dehydroxylation of GT8-66 approximates the stoichiometric amount of hydroxyl ion

Table 7. Proportion of rapidly extracted Mg, Al and Fe in two samples of glauconite

Sample	Percent of each ion removed at faster rate		
	Mg	Al	Fe
G294	3.2	7.1	4.6
G68A	27.3	10.7	50.3

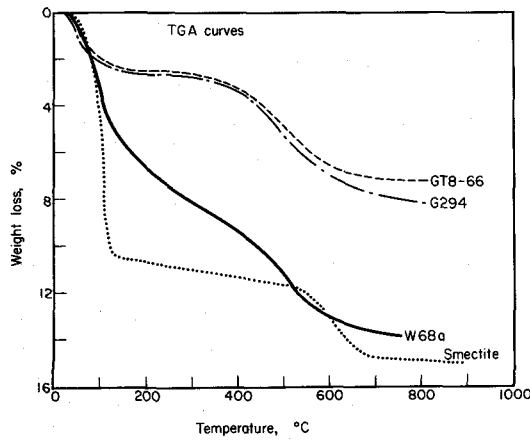


Fig. 5. Thermogravimetric analysis curves for sample GT8-66, G294, G68A, Smectite TGA curve is from Schultz (1971).

which should be present in such a glauconite (i.e. about 4.5 weight per cent). The 'dehydroxylation' weight loss of G294, for which an excess octahedral occupancy was calculated, when determined in the same way indicates a weight loss of 5.6 per cent over the same temperature interval, which is significantly in excess of the ideal 4.5 per cent, indicating the presence of excess OH.

The TGA curve for G68A is markedly different from either of the glauconites discussed above or the smectite, although its total weight loss is approximately that of the smectite. It is obvious that there is quite a large drop in weight at low temperatures which must reflect loss of interstitial and interlayer water. However, instead of leveling out at near constant weight, there is a continual rapid weight loss between about 130 and 700°C. It is suggested here that the large weight loss over this interval is caused by a combination of 2:1 octahedral layer (OH) loss over the temperature range 350–700°C—by analogy with GT8-66—and by (OH) loss from either extraneous or interlayer Mg, Fe and Al hydroxides

in the range of 130–350°C. The two dehydroxylation temperature ranges probably overlap but it is obvious that there is an anomalously very high weight loss in the temperature interval from about 150 to 400°C.

Without judging whether these hydroxyl groups are interlayer complexes or extraneous to the structure, it is now possible to recalculate the structural formulas for G68A and G294 after subtracting from the total analyses the proportions of Fe, Al and Mg that are removed in the dissolution experiments at the faster rate (Table 7). When this is done, the calculated octahedral occupancy of these two glauconites is within the probable limits of error of being ideally dioctahedral. Structural formulas for G68A and G294 are shown in Table 8. Therefore, various lines of evidence indicate that the apparent high octahedral occupancy in some glauconites can be accounted for by the presence of hydroxides.

EFFECT OF HEATING ON GLAUCONITE WITH EXCESS OCTAHEDRAL OCCUPANCY

To determine whether the hydroxides are coordinated as interlayer complexes in the expanded layers of the glauconite, or are extraneous to the glauconite structures, combined heating and X-ray diffraction studies were carried out on a magnesium-saturated specimen of sample G68A. The sample was heated to successively higher temperatures and then X-rayed at room temperature after heating. Under these conditions, a Mg-smectite with no interlayer hydroxy-complexes will rehydrate to two water layers after heating to temperatures of 200°C. At 330°C some layers will no longer expand and at 430°C all layers irreversibly contract to 9.5 Å. It can be seen from Table 9 that the layer spacing is significantly higher than 9.5 Å at even the highest temperature and that there is a progressive shift to lower d_{001} values with increasing temperature. This is interpreted as indicating the presence of interlayer metal-hydroxide

Table 8. Calculated structural formulas for G68A and G294, before and after subtraction of Fe, Al and Mg removed at faster rates by acid dissolution

	-0.44	-0.24	-0.68	+0.71
G294 Before	$\left[\text{Al}_{0.80}^{+3} \text{Fe}_{0.44}^{+2} \text{Fe}_{0.39}^{+2} \text{Mg}_{0.53} \right]_{2.16} (\text{Si}_{3.76} \text{Al}_{0.24})_{10} (\text{OH})_2 \left[\text{K}_{0.69} \text{X}_{0.02}^{+1} \right]$ <p style="text-align: center;">oct. cations</p>			
G294 After	-0.58	-0.21	-0.79	-0.73
	$\left[\text{Al}_{0.77}^{+3} \text{Fe}_{0.41}^{+2} \text{Fe}_{0.36}^{+2} \text{Mg}_{0.51} \right]_{2.05} (\text{Si}_{3.79} \text{Al}_{0.21})_{10} (\text{OH})_2 \left[\text{K}_{0.71} \text{X}_{0.02}^{+1} \right]$ <p style="text-align: center;">oct. cations</p>			
G68A Before	+0.13	-0.45	-0.32	-0.35
	$\left[\text{Al}_{0.97}^{+3} \text{Fe}_{0.72}^{+2} \text{Fe}_{0.01}^{+2} \text{Mg}_{0.52} \right]_{2.22} (\text{Si}_{3.55} \text{Al}_{0.45})_{10} (\text{OH})_2 \left[\text{K}_{0.15} \text{X}_{0.20}^{+1} \right]$ <p style="text-align: center;">oct. cations</p>			
G68A After	-0.24	-0.13		+0.37
	$\left[\text{Al}_{1.25}^{+3} \text{Fe}_{0.39}^{+2} \text{Fe}_{0.01}^{+2} \text{Mg}_{0.41} \right]_{2.06} (\text{Si}_{3.87} \text{Al}_{0.13})_{10} (\text{OH})_2 \left[\text{K}_{0.16} \text{X}_{0.21}^{+1} \right]$ <p style="text-align: center;">oct. cations</p>			

Table 9. Spacing of low angle reflection of G68A after heat treatment

Temperature	Heating Time (hrs.)*	d^{1001} "
150°	0.5	14.1
250°	0.5	13.6
350°	0.5	12.8
450°	1.0	11.2
500°	0.5	10.8

* The same specimen was heated to successively higher temperatures.

layers as suggested above and described by Rich (1968) and Van der Marel (1964).

It is therefore concluded that the high octahedral occupancies reported for many glauconites are attributable to the presence of interlayer hydroxy complexes of Mg, Al and Fe. Any consideration of compositional-structural relationships in glauconite must take this feature into account.

The structural formulas of aluminous illite-smectite from sedimentary rocks (Hower and Mowatt, 1966) indicates that the occurrence of interlayer hydroxy-metal complexes seems to be far less common in those minerals than in glauconite. A consideration of proposed mechanisms of glauconite genesis leads to a reasonable explanation for this difference. The process of glauconitization (Burst, 1958a, b; Takahashi and Yagi, 1929) involves, among other factors, an environment in which iron is mobilized. Mobilization of iron is also an important factor in soil development and hydrated clays of many varieties frequently contain large amounts of interlayer iron hydroxide. We believe that, as in soils, the presence of important amounts of interlayer iron hydroxide in glauconite is attributable to the mobilization of iron. To us, the most plausible explanation for the mobility of iron appears to be that given by Huang and Keller (1972), for processes of soil formation, in which complexing with organic acids greatly increases the mobility of iron and aluminum. The influence of organic material in the glauconitization process has long been thought to be important (Burst, 1958a).

We suggest that the mobilization of iron and aluminum by organic complexing during glauconitization explains the frequent formation of interlayer hydroxy-metal complexes. Such a process is significantly less likely in the formation of aluminous illite-smectite, much of which probably forms under the conditions of burial diagenesis (Perry and Hower, 1970) and thus intergrade iron and aluminum are much less common.

PROGRESSIVE DISSOLUTION DATA FOR POTASSIUM IN GLAUCONITE

The results of a progressive acid dissolution study of potassium in glauconite are reported in detail by Thompson and Hower (1973). Figure 6 is typical of the results obtained for potassium. The top curve labeled 'total K' shows a linear relation at dissolution times greater than about 10 hr. The straight line nature

of the curve at longer times indicates that the potassium which is being removed in that longer time interval is held in the mineral in a specific structural position. The curved nature and steeper slope of the extraction at shorter times indicates a contribution to the extraction rate by potassium which is being removed at a much higher rate. The lower curve labeled 'fast K' is the result of the first deconvolution of the curve for total potassium and shows except at shortest times, a straight line relationship. Again the straight line relationship implies that some of the potassium is held in a different, but specific structure position, with the remaining amount (the non-linear portion of the curve after the first deconvolution) indicating at least one more potassium lattice position.

The dissolution curve for sample G68A, then, has three separate parts. Initially potassium is removed at a very, very high rate. This potassium is readily interpretable as exchangeable potassium. The potassium which is extracted at the longest dissolution times and plots along a straight line in the total K vs time curve is that which is extracted most slowly and presumably occupies the 6-fold coordination site (distorted 12-fold site) in the collapsed interlayer positions of the glauconite. It is difficult to assign a structural site to the potassium which is removed at the intermediate rate; that it occupies a specific site is certain for it is removed at a constant rate. We suggest that the potassium extracted at the intermediate rate is present in the hydrated layers along with the exchange potassium but is present in the hexagonal voids surrounded by 6 oxygens. This potassium would occupy the same plane as the basal oxygens of the tetrahedral layer as suggested by Marshall

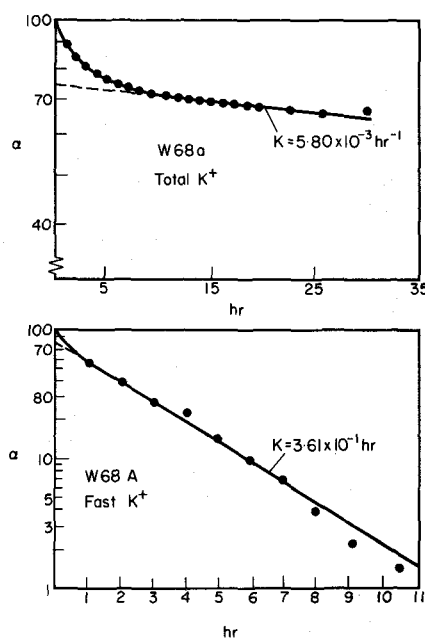


Fig. 6. Acid dissolution curves for potassium in sample G68A. α = fraction of potassium remaining in solid; α^1 = fraction of potassium removed at a fast rate (determined by subtracting straight line portion from 'Total K' curve) remaining in solid.

(1964) and Mering and Glaesser (1954) for sodium in smectite. It is consequently much more difficult to remove than normal exchange ions.

The determination that a significant proportion of potassium is located in expandable interlayer positions in some glauconites is of considerable importance in the radiometric dating of glauconite pellets. In calculating the K^+ occupancy of the illite layers in the mineralogy section, we assumed that no K^+ was present in the smectite layers. The quantity of K^+ in the smectite layers is such that its presence in smectite layers does not materially alter the structural argument, but is very important for radiometric dating purposes. Daughter products of radioactive elements located in expandable interlayer positions would be totally lost from the glauconite structure. We suggest that the loss of daughter products from such sites causes the systematically low radiometric ages from glauconites which has been noted previously in the literature (Hurley *et al.*, 1960). It is possible to correct for errors thus caused in radiometric age determinations by using acid dissolution to determine the relative abundance of potassium or rubidium in each of the three lattice sites, and recalculating the age using only the amount of the parent element in the illite layers. (Thompson and Hower, 1973).

SUMMARY OF CONCLUSIONS

(1) Calculated X-ray powder diffraction patterns of iron-rich illite-smectite structures generated by the method of Reynolds and Hower (1970) resemble X-ray diffraction patterns of glauconite quite well. We conclude that glauconite structures are identical to the structures of mixed layer illite-smectites.

(2) The structural variations in glauconite are:

- (a) glauconite covers the range from less than 5 to at least 65 per cent smectite layers,
- (b) glauconite with more than 25 per cent smectite layers is randomly interstratified,
- (c) almost all samples of glauconite which have 10–25 per cent smectite layers show allevardite-type ordered interstratification of the illite and smectite layers and
- (d) glauconites with 10 per cent or fewer smectite layers, and some with 15 per cent expandable layers, show ordering of the IMII type.

(3) An excellent relationship exists between the number of potassium atoms per unit cell and the proportion of illite layers in glauconite. This relation indicates a continuous mineralogical series, analogous to that of aluminous mixed-layer illite-smectite.

(4) As the proportion of illite layers in glauconite increases the mean potassium content of the illite layers also increases. We interpret this to mean that as expandability decreases a higher structural charge and a higher potassium content are required to form illite layers from the remaining smectite layers. Sawhney's (1967) model for the conversion of vermiculite to mica layers on potassium absorption adequately

explains both this phenomenon and the occurrence of ordered interlayering in glauconites (and aluminous illite-smectite) with high proportions of illite layers.

(5) The illite layers in glauconite of high expandability are much lower in interlayer charge and potassium content than are the illite layers in structurally equivalent aluminous illite-smectite. This feature can be explained by the greater stability of potassium ions in the voids of the basal plane of glauconite because of its 1M structure and, perhaps, to the presence of large amounts of octahedral iron. Giese (1973) has shown that the tilt of the O-H axis away from the (001) plane in the 1M structure is greater than for any other polymorph, thus minimizing the electrostatic repulsion of interlayer potassium by hydrogen. The lower electronegativity of iron may allow an even greater tilt of the O-H axis, allowing a particularly stable bonding environment for potassium in glauconite.

(6) The apparent octahedral occupancy in excess of two cations per three octahedral sites shown by some glauconites is attributed to the presence of hydroxy-complexes of magnesium, aluminum, and iron in the expandable layers. The amounts of these interlayer hydroxy-complex iron, aluminum and magnesium can be determined by acid dissolution studies.

(7) Low radiometric ages from some glauconite pellet samples are attributable in part or in whole to the presence of potassium in expanded layers of the glauconite structure from which sites radiogenic daughter products would predictably be readily lost. Corrections can be made in age calculations using techniques of acid dissolution.

Acknowledgements—The writers thank Robert C. Reynolds for his help in preparing the calculated X-ray diffraction patterns. We thank R. G. Douglas, W. Pratt, J. D. Obradovich, C. Rainwater, F. G. Stehli and E. G. Wermund for sample donations. W. R. Cook, Jr. kindly performed some of the thermogravimetric analyses. Samuel M. Savin critically read the manuscript and offered many improvements.

REFERENCES

- Barackman, M. A. (1964) A study of the mineral glauconite in Apalachicola Bay, Florida: Thesis, Florida State University, Tallahassee, Florida, p. 44 (unpublished).
- Bassett, W. A. (1960) Role of hydroxyl orientation in mica alteration: *Bull. Geol. Soc. Am.* **71**, 449–455.
- Bell, D. H. and Goodell, H. G. (1967) A comparative study of glauconite and the associated clay fraction in modern marine sediments: *Sedimentology* **9**, 169–202.
- Bentor, Y. K. and Kastner, M. (1965) Notes on the mineralogy and origin of glauconite: *J. Sediment. Petrol.* **35**, 155–166.
- Brindley, G. W. and Youell, R. F. (1951) A chemical determination of 'tetrahedral' and 'octahedral' aluminum ions in a silicate: *Acta Cryst.* **4**, 495–496.
- Brown, G. (1961) (Editor) *The X-ray Identification and Crystal Structures of Clay Minerals*. Mineralogical Society (Clay Minerals Group), London.
- Burst, J. F. (1958a) 'Glauconite' pellets: Their mineral nature and applications for stratigraphic interpretations: *Bull. Am. Ass. Petrol. Geologists* **42**, 310–327.

- Burst, J. F. (1958b) Mineral heterogeneity in 'glaucinite' pellets. *Am. Miner.* **43**, 481-497.
- Cloos, P., Gastuche, M. C. and Groegart, M. (1961) Cinétique de la destruction de la glauconite par l'acide chlorhydrique étude préliminaire: *Int. Geol. Cong. 21st Rept. Session*, Norden, 35-50.
- Ehlmann, A. J., Hulings, N. C. and Glover, E. D. (1963) Stages of glauconite formation in modern foraminiferal sediments: *J. Sediment. Petrol.*, **33**, 87-96.
- Foster, M. D. (1951) Geochemical studies of clay minerals—I. The importance of exchangeable magnesium and cation exchange capacity in the study of montmorillonitic clays: *Am. Miner.* **36**, 717-730.
- Giese, R. F. (1971) Hydroxyl orientation in muscovite as indicated by electrostatic energy calculations: *Science* **172**, 263-264.
- Giese, R. F. (1973) Hydroxyl orientations—dioctahedral micas. *22nd Ann. Clay Minerals Conf.*, Banff, Alberta, Canada, October 7-11.
- Granquist, W. T. and Sumner, G. G. (1957) Acid dissolution of a Texas bentonite: *Clays and Clay Minerals* **6**, 292-301.
- Gruner, J. W. (1935) The structural relations of glauconite and mica: *Am. Miner.* **20**, 699-714.
- Grim, R. E., Bradley, W. F. and Brown, G. (1951) The mica clay minerals. In: *X-ray identification and crystal structures of clay minerals*, Brindley, G. W. (Editor) The Minerals Soc. pp. 138-172.
- Gupta, G. C. and Malik, W. U. (1969a) Chloritization of montmorillonite by its coprecipitation with magnesium hydroxide: *Clays and Clay Minerals* **17**, 331-338.
- Gupta, G. C. and Malik, W. U. (1969b) Fixation of hydroxy-aluminum by montmorillonite: *Am. Miner.* **54**, 1625-1634.
- Hendricks, S. B. and Ross, C. S. (1941) Chemical composition and genesis of glauconite and celadonite: *Am. Miner.* **26**, 683-708.
- Hower, J. (1961) Some factors concerning the nature and origin of glauconite. *Am. Miner.* **46**, 313-334.
- Hower, J., Schmittroth, L. A., Perry, E. C. and Mowatt, T. C. (1965) X-ray spectrographic major constituent analysis in undiluted silicate rocks and minerals (abs.): *Geol. Soc. Am. Spec. Paper* **82**, 96-97.
- Hower, J. and Mowatt, T. C. (1966) The mineralogy of illites and mixed-layer illite-montmorillonite: *Am. Miner.* **51**, 825-854.
- Huang, W. H. and Keller, W. D. (1972) Geochemical mechanics for one dissolution, transport and deposition of aluminum in the zone of weathering: *Clays and Clay Minerals* **20**, 69-74.
- Hurley, P. M., Cormier, R. F., Hower, J., Fairbairn, H. W. and Pinson, Jr., W. H. (1960) Reliability of glauconite for age measurement by K-Ar and Rb-Sr methods: *Bull. Am. Ass. Petrol. Geologists*, **11**, 1793-1808.
- Kinter, E. B. and Diamond, S. (1956) A new method for preparation and treatment of oriented-aggregate specimens of soil clays for X-ray diffraction analysis: *Soil Science* **81**, 111-120.
- MacKenzie, R. D. (1970) *Differential Thermal Analysis*, Academic Press, New York.
- McRae, S. G. (1972) Glauconite: *Earth-Sci. Rev.* **8**, 397-440.
- Manghni, M. H. and Hower, J. (1964) Glauconites: Cation exchange capacities and i.r. spectra—II. The cation exchange capacity of glauconite: *Am. Miner.* **49**, 586-598.
- Marshall, C. E. (1935) Layer lattices: *Z. Kristallog.* **91**, 443-449.
- Marshall, C. E. (1964) *The Physical Chemistry and Mineralogy of Soils*, Vol. I, Wiley, New York.
- Mering, J. and Glaesser, R. (1954) Sur le rôle de la valence des cations échangeables dans le montmorillonite: *Bull. Soc. France. Miner.* **77**, 519-530.
- Osthaus, B. (1954) Chemical determination of tetrahedral ions in nontronite and montmorillonite: *Clays and Clay Minerals* **2**, 404-417.
- Osthaus, B. (1965) Kinetic studies on montmorillonites and nontronite by the acid dissolution techniques: *Clays and Clay Minerals* **4**, 301-321.
- Perry, E. A. and Hower, J. (1970) Burial diagenesis in Gulf Coast, pelitic sediments: *Clays and Clay Minerals* **18**, 165-177.
- Pratt, W. L. (1962) The origin and distribution of glauconite from the sea floor off southern California. Thesis, University of Southern California, Los Angeles, Calif., 285 pp. (unpublished).
- Reichen, L. E. and Fahey, J. J. (1962) An improved method for the determination of FeO in rocks and minerals including garnet: *U.S. Geol. Surv. Bull.* **1144-B**, 1-5.
- Reynolds, R. C. and Hower, J. (1970) The nature of interlayering in mixed-layer illite-montmorillonites: *Clays and Clay Minerals* **18**, 25-36.
- Rich, C. I. (1968) Hydroxy interlayers in expandable layer silicates: *Clays and Clay Minerals* **16**, 15-30.
- Ross, G. S. (1969) Acid dissolution of chlorites: Release of magnesium, iron and aluminum and mode of acid attack: *Clays and Clay Minerals* **17**, 347-354.
- Sawhney, B. L. (1967) Interstratification in vermiculite: *Clays and Clay Minerals* **15**, 75-84.
- Schneider, H. (1927) A study of glauconite: *J. Geol.* **35**, 289-310.
- Schultz, L. G. (1971) Lithium and potassium absorption, dehydroxylation temperature and structural water content of aluminous smectites: *Clays and Clay Minerals* **17**, 115-150.
- Takahashi, J. I. and Yagi, T. (1929) Peculiar mud grains and their relation to the origin of glauconite: *Econ. Geol.* **24**, 838-854.
- Thompson, G. R. and Hower, J. (1973) An explanation for low radiometric ages from glauconite: *Geoch. et Cosmoch. Acta* **37**, 1473-1492.
- Triplehorn, D. M. (1966) Morphology, internal structure and origin of glauconite pellets: *Sedimentology* **6**, 247-266.
- Tsuboi, M. (1950) On the positions of the hydrogen atoms in the crystal structure of muscovite as revealed by infrared absorption study: *Bull. Chem. Soc. Japan* **23**, 83-88.
- Van der Marel, H. W. (1964) Identification of chlorite and chlorite-related minerals in sediments: *Beit. z. Mineral. Petrograph.* **9**, 462-480.
- Vedder, W. and McDonald, R. S. (1963) Vibrations of the OH ions in muscovite: *J. Chem. Phys.* **38**, 1583.
- Warshaw, C. M. (1957) The mineralogy of glauconite. Thesis, Pennsylvania State Univ., University Park, PA, p. 155.
- Weaver, C. E. (1965) Potassium content of illite: *Science* **147**, 603-605.
- Yoder, H. S. (1959) Experimental studies on micas, a synthesis: *Clays and Clay Minerals* **6**, 42-60.